ELSEVIER

Journal of Nuclear Materials 296 (2001) 43–53

journal of nuclear materials

www.elsevier.com/locate/jnucmat

Status of the first SINQ irradiation experiment, STIP-I

Y. Dai *, G.S. Bauer

Spallation Neutron Source Division, Paul Scherrer Institut, 5232 Villigen PSI, Switzerland

Abstract

The irradiation program at SINQ was initiated in 1996 in collaboration with Commissariat à l'Energie Atomique Centre d'Etudes de Saclay (CEA), Forschungszentrum Jülich (FZJ), Japanese Atomic Energy Research Institute (JAERI), Los Alamos National Laboratory (LANL) and Oak Ridge National Laboratory (ORNL). The first irradiation experiment (STIP-I) was carried out from July 1998 to December 1999 in SINQ target MARK-II, which received total charge of 6.8 A h of protons with a peak fluence of 3.2×10^{25} p/m^2. In this experiment more than 1500 samples of different types of Fe-, Al-, Zr-, Ni-, Ti-, W-, Mo-based alloys and their weld materials were irradiated. At the same time, 101 dosimetry detectors of Al, Au, Co, Cu, Fe, Ni, Nb and Ti were placed close to the samples in order to analyse the spallation spectrum at different positions. In addition, there were 11 rods from austenitic and martensitic steels and Zircaloy-2, 3 tubes of Zircaloy-2 and 7 lead (Pb) filled tubes of 9Cr–1Mo irradiated for different testing purposes, which would also be available for the post-irradiation examination (PIE). The irradiated samples have been retrieved and will be tested soon by different laboratories. The main results of the PIE should be available in 2001.

1. Introduction

A number of activities are being carried out at SINQ to study the change of mechanical properties and microstructures of structural materials in an environment representative for spallation neutron source. This relates to both, radiation effects and liquid metal corrosion in liquid metal targets [1,2]. The present irradiation program is one of the key activities which aims at studying radiation damage produced in structural materials by a spallation spectrum, i.e. high-energy protons plus spallation neutrons, in a realistic time history.

The SINQ target-irradiation program (STIP) was initiated in 1996 and conducted under a collaboration with Forschungszentrum Jülich (FZJ), Oak Ridge National Laboratory (ORNL), Commissariat à l'Energie Atomique Centre d'Etudes de Saclay (CEA), Japanese Atomic Energy Research Institute (JAERI) and Los Alamos National Laboratory (LANL).

The program planning was done in co-ordination with a similar and even larger irradiation program at LANL [3]. The first STIP (STIP-I) would provide information on mechanical properties and microstructure of about 40 kinds of materials irradiated in a wider temperature range from 70°C to 410°C. The program was focused on: (a) comparison between different type of alloys of the same base; (b) investigation on welded materials; and (c) study on advanced low-activation martensitic/ferritic steels developed by fusion materials community.

In this paper the detailed information on materials selection, specimen geometry, irradiation parameters and PIE program will be described.

2. Materials selection

The selection of candidate materials for the container of a liquid metal target was studied based on the knowledge obtained by the fusion materials community. Both martensitic and austenitic steels are considered to be the best ones [4–6]. Therefore, in the present irradiation program emphasis was on these two classes of steels. For wider interests other materials applied in the

* Corresponding author. Tel.: +41-56 310 4171; fax: +41-56 310 2485.

E-mail address: yong.dai@psi.ch (Y. Dai).

0022-3115/01/$ - see front matter
PII: S0022-3115(01)00544-X

existing spallation sources or proton-irradiation facilities have been also included in this irradiation program.

2.1. Austenitic steels

AISI 316L is the best understood austenitic stainless steel with a large data base for neutron irradiation. Several other types with different kinds of modifications were also well studied with neutron irradiation, which include the Japanese versions, JPCA and 316F. Thus, AISI 316L was selected as the representative austenitic steel and JPCA and 316F were included for comparison.

Cold-worked (CW) austenitic steels have much higher yield strength and lower irradiation swelling than the solution-annealed (SA) ones, although they have limitations for weld structures. CW 316L and CW 316F were irradiated for comparison with SA 316L and SA 316F.

2.2. Martensitic steels

9Cr–1Mo(mod.) is a well studied martensitic steel in the fusion community and was taken as representative for conventional martensitic steels. Russian steel, I3XI3C2M2, and French steel, EM10, were included for comparison. In the last decade, low-activation martensitic steels (LAMS) have been developed, which are attractive for their good fracture behaviour after neutron irradiation. There are several versions developed by different countries. One of them, F82H(mod), developed in Japan was selected by IEA as a common material studied world-wide in the fusion materials community. Since PSI included about 200 samples in the APT irradiation experiment, F82H was used as a reference material only in STIP-I. The German version, Optifer, was selected as the representative for the LAMS and the Swiss version, Optimax, was also included for comparison.

2.3. Other alloys

In the existing spallation neutron sources, Al-, Zr- and Ni-based alloys are also frequently employed. For example, Al-alloy $AlMg_3$ is used for the safety hull material and Zircaloy-2 is used as target materials in SINQ, and Inconel 718 is used as the window material in LANSCE. In the proton-irradiation facility PIREX at PSI a Ti-based alloy is used for the sample cooling tube which is directly exposed to the proton beam. Therefore, Al-, Zr-, Ni- and Ti-based alloys were also included in the irradiation. Furthermore, refractory materials, W and Mo and their alloys, were selected for for their potential applications in future high-power accelerator driven systems.

2.4. Weld materials

Weld structures cannot be avoided in a spallation neutron source target. It is, therefore, necessary to study the behaviour of weld materials after irradiation. Electron-beam weld (EBW) materials were selected as the main object for investigation. Tungsten-inert-gas weld (TIG) and laser weld (LW) materials were also included for comparison. In weld materials the width of the weld-zone and heat-affected-zone depends on the thickness of the plates to be welded. The wall of the liquid metal target container is about 3 mm thick. So it is important to study welds of about 3 mm thickness. These 3 mm thick welds will be compared with well studied 15–30 mm thick weld materials obtained from the fusion materials community. In this irradiation program, EBW and TIG samples from plates of 316L, 9Cr–1Mo, Optifer, F82H, Inconel 718, Al-alloy AG3 of different thickness, and laser weld samples of Zircaloy-4 were included.

The selected materials are listed in Table 1 which presents the irradiation matrix. Chemical compositions of the materials are given in Table 2.

3. Specimens

3.1. Specimen geometry

The SINQ target MARK-I was a matrix of about 490 Zircaloy-2 rods and tubes of 10.75 mm diameter welded into a hexagonal case of Zircaloy-2. To irradiate specimens in this kind of target, special rods were designed to replace normal target rods. The specimens had to be packed in tubes. In order not to introduce difficulty in predicting effects on the cooling water chemistry, tubes of Zircaloy-2 were used. These tubes had an outer diameter of 10.75 mm and an inner diameter of 9.25 mm. Therefore the cross-section of specimens was mainly limited by this inner diameter. On the other hand, since the proton beam had roughly a two-dimensional Gaussian distribution with $\sigma_x = 2.12$ and $\sigma_y = 3.56$ cm, the specimens had to be as short as possible to avoid large dose variation along their length. In addition, the specimens should be close packed for good heat transfer. As a consequence of all these factors, only small (or miniature) flat types of specimens could be used.

Fortunately, the small specimen technology has been studied in the fusion materials community and the same concepts could be directly applied to our context without or with little modification [7]. The STIP collaboration agreed to use seven types of specimens to obtain results on different properties of materials:

1. 3 mm diameter TEM discs of 0.25 mm thickness were used to provide information on microstructure.

Table 1
SINQ irradiation matrix[a]

	Materials	ID	Tensile	Bend-fatigue	Tear	Bend-bar	Charpy	Shear punch	TEM	
1	SA 316L	A	32	10	10	7		40	15	
2	CW 316L	B	26	9	5	7		24	11	
3	316L EBW	C	23	6	5				11	
4	EC316LN EBW*	D	20	6	5				11	
5	EC316LN TIG	E	20	6	5				10	
6	EC316LN	J	18	7	5	3			10	
7	SA JPCA	F	9	6	5				6	
8	SA 316F	G	18	6	5				8	
9	CW 316F	H	12						2	
10	9Cr–1Mo	I	26	9	12	6	8	40	11	
11	9Cr–1Mo EBW*	K	18	6	5	3			13	
12	9Cr–1Mo TIG	L	19	6	5				11	
13	Optifer	M	26	9	13	9	12	44	13	
14	Optifer EBW*	O	18	6	5	2			12	
15	Optimax A	N	16	6	5	5	8	24	11	
16	Optimax C	IG	18				8		6	
17	F82H	P	23	8	10	6	8	40	12	
18	F82H TIG	Q	9	6	5				6	
19	F82H EBW	R	9	6	5				6	
20	F82H EBW*	S	20	6					8	
21	I3XI3C2M2	T	9	4	5				8	
22	EM10/ME	ID	16						6	
23	EM10/MR	IE	14						4	
24	EM10/MT	IF	16						5	
25	Al 6061-1	U	6	3					5	
26	Al 6061-3	U	9	3					5	
27	AG3-2	V	15	3	5				9	
28	AG3-7/1	V	9	3	5				7	
29	AG3-3(EBW**)	W	5	3					5	
30	AG3-7/2(EBW**)	W	5	3					5	
31	Zircaloy-4	X	14	6	5				11	
32	Zircaloy-4 LW	Y	11	6					5	
33	Inconel 718	IH	17						7	
34	Inc. 718 EBW*	II	14						7	
35	Ti–Zr	Z	8				4		14	
36	W	IA	5					10	4	
37	W–5% Re	IB	7					10	4	
38	W–26% Re	IC	8					10	5	
39	Mo	IJ	6					8	7	
40	Mo–W	IK	6					8	7	
	Sum		580	158	130	48	48	258	323	Sum 1545
	Dosimetry									
1	Al		44							
2	Au		6							
3	Cu		19							
4	Co		6							
5	Fe		7							
6	Nb		7							
7	Ni		6							
8	Ti		6							
	Sum		101							Total 1646

[a] Note: EBW – electron-beam weld from thick (⩾15 mm) plates; EBW* – EB weld from 3 mm thick plates; EBW** – EB weld from 0.4 mm thick plates; TIG – Tungsten-inert-gas weld; LW – laser weld.

Table 2
Chemical compositions of austenitic steels, martensitic steels, Al-based alloys, Zircaloy-4, Inconel 718, and Ti-alloys

(*a*) *Austenitic steels*

Steel	Fe	Cr	Ni	Mo	Mn	Ti	Co	Cu	B	C	Si	P	S	N	Ta
AISI 316L	Bal.	17.17	12.24	2.31	1.75	–	0.077	0.07	0.0009	0.019	0.35	0.02	0.0007	0.073	0.002
EC316LN	Bal.	17.45	12.2	2.5	1.81	–				0.024	0.39	–		0.067	
JPCA	Bal.	14.14	15.87	2.29	1.54	0.22	0.028		0.004	0.058	0.50	0.026	0.004	0.003	
316F	Bal.	16.79	13.95	2.34	0.23	–	<0.001	<0.01	–	0.040	0.04	<0.003	0.002	0.011	

(*b*) *Martensitic steels*

Steel	Fe	Cr	Ni	Mo	Mn	Ti	V	Nb	W	Ta	Cu	C	Si	P	S	N
9Cr–1Mo	Bal.	8.32	0.09	0.86	0.48	0.001	0.20	0.06	<0.01		0.03	0.092	0.15	0.012	0.004	0.055
Optifer	Bal.	9.48	0.06	0.002	0.55		0.245		0.985	0.065		0.125	0.04	0.0015	0.003	
F82H	Bal.	7.87	0.02	0.003	0.1	0.004	0.19	0.0002	1.98	0.03	0.01	0.09	0.07	0.003	0.001	0.007
Optimax A	Bal.	9.3	<0.01	0.09	0.60	<0.01	0.24	<0.01	0.97		<0.01	0.098	0.02	0.01	<0.001	0.001
Optimax C	Bal.	9.5	<0.01	0.15	0.40	<0.01	0.25	<0.01	1.9		<0.01	0.11	0.03	0.011	<0.001	0.007
I3XI3C2-M2	Bal.	12.4	0.22	1.49	0.32							0.19	1.70	0.014	0.009	
EM10	Bal.	8.76		1.05	0.48							0.105	0.37	0.016	0.003	

(*c*) *Al-based alloys* (*wt%*, **ppm*)

Alloy	Al	Si	Fe	Cu	Mn	Mg	Cr	Ni	Zn	Ti	Zr	PbC	S
Al-6061	Bal.	0.59	0.475	0.21	0.10	0.995	0.17		0.01	0.01			
AG3	Bal.	0.15	0.26	50*	0.27	2.78	0.18	20*	0.01	0.02	20*	30*	4*

(*d*) *Zircaloy-4* (*wt%*, **ppm*)

	Zr	Cr	Fe	Sn	O	Al	C	H	Hf	N	Si	Nb	Ni	P	V
Zircaloy-4	Bal.	0.11	0.21	1.43	0.125	20*	100*	3*	51*	31*	34*	<50*	<40*	<15*	<20*

(*e*) *Inconel 718* (*wt%*, **ppm*)

	Ni	Cr	Fe	Sn	O	Al	C	H	Hf	N	Si	Nb	Ni	P	V
Inconel 718	Bal.	0.11	0.21	1.43	0.125	20*	100*	3*	51*	31*	34*	<50*	<40*	<15*	<20*

(*f*) *Ti-alloys* (*wt%*, **ppm*)

	Ti	Zr	C	O	N	H	Fe	Ni	Cr
Ti–5Zr	Bal.	4.90	0.017	0.080	0.004	0.0024	0.02	0.015	0.011
Ti–22Zr	Bal.	21.7	0.006	0.068	0.009	0.0023	0.020	0.015	0.011

2. The same size of discs were used for small-punch (SP) tests which could provide useful information on tensile and fracture properties.
3. Miniature tensile specimens of only 12 mm length were included for tensile properties.
4. Miniature bend-fatigue specimens were selected to obtain fatigue properties.
5. So called tear test specimens were used to obtain some qualitative information of fracture properties.
6. Small bend-bar specimens were selected to get quantitative information of fracture toughness of a few kinds of materials.
7. 1/3 size charpy specimens were selected to get information on ductile–brittle transition temperature (DBTT) of a few kinds of materials.

The shapes and dimensions of the specimens are illustrated in Fig. 1.

3.2. Specimen preparation

Specimens were prepared by different participating laboratories based on their own request and then collected at PSI. Most of the specimens were marked at PSI with either laser or spark inscription technique. After marking, all specimens were re-polished slightly with polishing papers of No. 2000 to remove the pile-ups of welded materials that occurred during marking in order to reduce the gaps between specimens when packed together. Then the dimensions of the samples were measured.

In particular, the bend-bar samples were manufactured by different suppliers but were pre-cracked at PSI. All charpy specimens were prepared by PSI to ensure uniform specimen dimensions, especially for the notches. The materials Optifer and 9Cr–1Mo were obtained from FZJ and ORNL, respectively.

Detailed information on preparation of each kind of specimen can be found in a technical report [8].

3.3. Dosimetry specimens

In order to evaluate the neutron and proton spectra of the irradiation, 3 mm diameter discs of pure Al, Au, Cu, Co, Fe, Ni, Nb and Ti were used as detectors. These discs were about 0.15 mm thick. They were stacked together at some positions. Between each two discs, thin foils of 20 μm thickness of the same material (for Al, Au, Cu, Fe, Nb) or Al (for Co, Ni, and Ti) were inserted to stop high-energy recoils between the discs. Al and Cu discs were placed throughout the specimen rods to determine the dose distribution.

3.4. Specimen loading

Tensile, bend-fatigue, tear and TEM/SP samples were packed in two layers in a specimen carrier. Five such specimen carriers were sandwiched in a specimen bed, then slipped into a Zircaloy-2 tube as illustrated in Figs. 2 and 3. The material of the specimen carriers was 316L and the material for the specimen beds was Zircaloy-2. Fig. 4 gives an example demonstrating what was irradiated in one rod, while Fig. 5 shows two layers after loading in the specimen carriers.

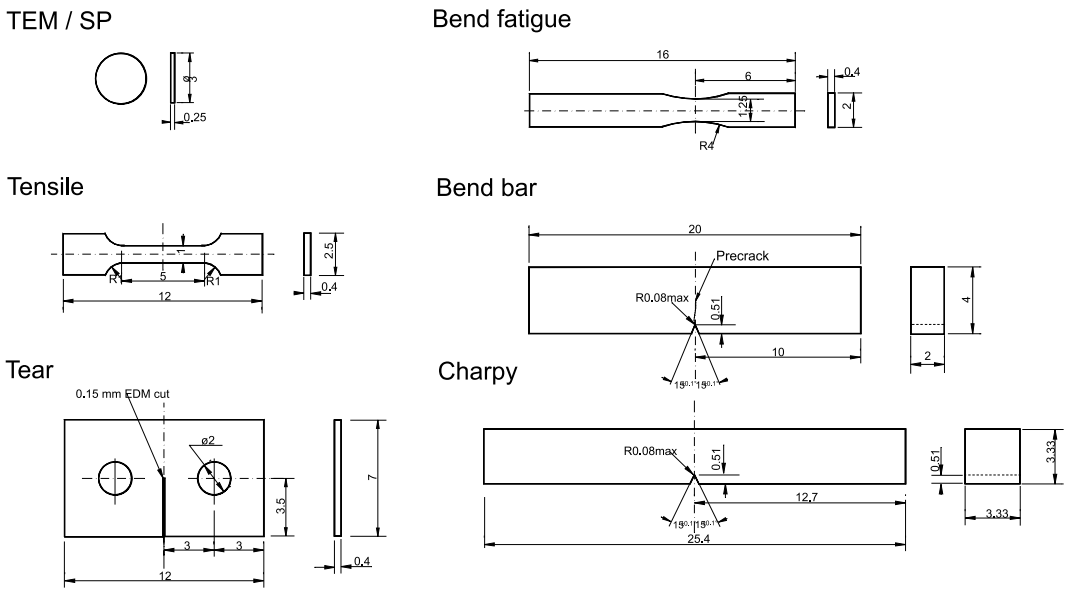

Fig. 1. Drawings of the specimens irradiated in SINQ target MARK-II. All dimensions in mm.

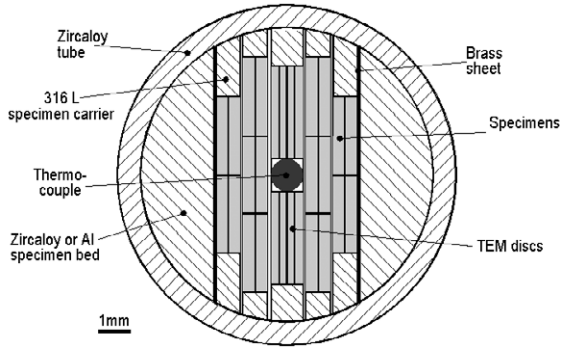

Fig. 2. Sketch showing the cross-section of one specimen rod.

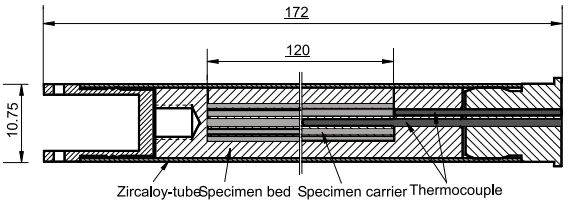

Fig. 3. Sketch showing the layout of specimen rods 1, 4 and 10.

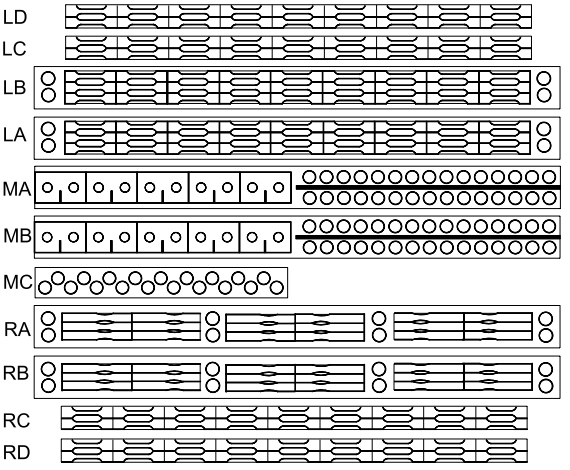

Fig. 4. Specimen layout in a rod contains tensile, tear, SP, TEM and dosimetry samples. The marks from LD to RD corresponds to the layers from left to right in Fig. 2.

Bend-bar and charpy specimens were simply packed in specimen beds of $AlMg_3$ and then slipped into Zircaloy-2 tubes. In one rod, 16 bend-bar or charpy samples could be irradiated at two doses. Therefore, it is possible to have 8 charpy samples of the same dose to make a complete DBTT test.

In total, 10 rods with test samples were prepared. They contained 1646 samples, of which 580 are tensile samples, 158 bend-fatigue samples, 130 tear-test samples, 48 bend-bars, 48 charpy samples, 258 SP samples, 323 TEM discs and 101 dosimetry discs. The detailed information of the irradiation matrix is present in Table 1.

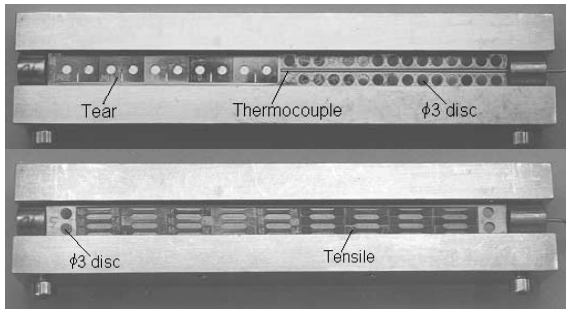

Fig. 5. View of samples packed in two specimen beds.

As can be seen in Fig. 4, there are large gaps between two adjacent tensile specimens at the gauge section. This may give rise to an inhomogeneous temperature distribution due to a poor heat transfer. To minimise this effect, small fillers of 316L and aluminium with a shape similar to the gaps were cut and placed in the gaps between the tensile specimens.

All the pieces, namely the specimens, small fillers, specimen beds, specimen carriers and Zircaloy tubes, were cleaned in acetone in an ultrasonic bath before loading. After loading the sample packages, the tubes were sealed with laser welding in a chamber filled with 2 bars of He gas. Therefore all tubes contain a small amount of He gas at 2 bars. For measuring irradiation temperatures, a total of 6 thermocouples were installed in 3 of the 10 rods (2 thermocouples in each rod).

3.5. Other samples

In order to have specimens available for studies with neutron scattering, 6 rods of 9.3 mm diameter of SA 316L, CW 316L, 9Cr–1Mo and F82H were inserted into either Zircaloy-2 or 9Cr–1Mo tubes. Another 7 rods consisted of 9Cr–1Mo tubes filled with Pb (this latter kind of rods served as target rods for the present SINQ target MARK-III, where they are used instead of Zircaloy-2 to increase the neutron intensity). These 13 rods were sealed in the same way as described above. All special rods were held in place in the target with wire locks for removal after irradiation (Fig. 6). In addition, there were 5 Zircaloy-2 rods and 3 Zircaloy-2 tubes fixed in the same way for later examination. There are 2 thermocouples located at the centre points of rod ZR1 and rod L.

The positions of all these special rods were in the central columns of the target as illustrated in Figs. 6 and 7. The contents for each rod are given in Table 3.

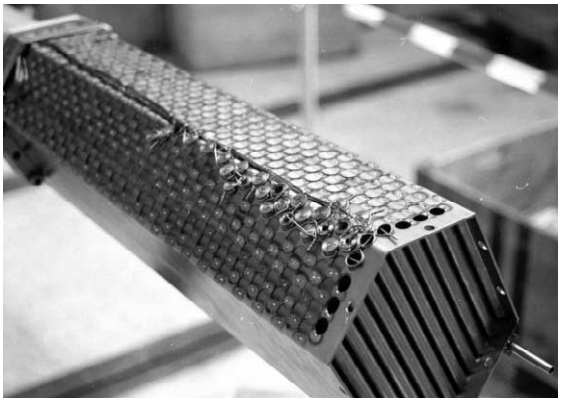

Fig. 6. Photograph of SINQ target MARK-II before irradiation, showing the bulk of the Zircaloy-2 rods and tubes welded in place and the specimen rods fixed by wire locks. The bulk is 565 mm long.

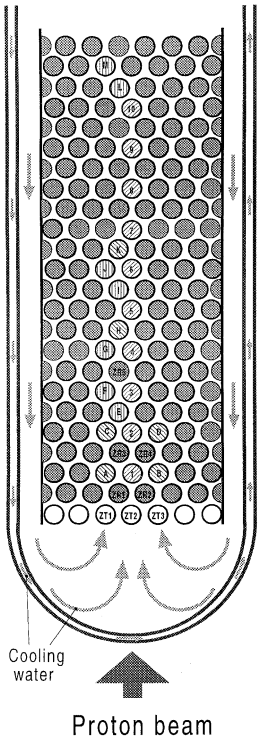

Fig. 7. Sketch showing the positions of specimen rods in the lower part of the target. The contents of the rods are given in Table 3. Note that there are actually 9 or 10 rods in one row, see Fig. 6.

4. Irradiation dose

The proton and neutron flux at the different positions in the target has been calculated using the LAHET code [9,10]. Fig. 8(a) shows the proton spectra at the centre positions of the 10 specimen rods. Fig. 8(b) giving the neutron spectra at the centre positions of Rod 1, Rod 5 and Rod 10. It can be seen that with increasing penetration depth, the energy of the protons decreases and the width of the proton spectra broadens. For the neutron spectra, the low-energy part changes little, but the high-energy neutron flux decreases with increasing depth in the target. The proton and fast-neutron spectra are almost the same along the axis of each rod but decrease in intensity due to the intensity profile of the beam. Figs. 9(a) and (b) illustrate the total fluences of protons and fast neutrons (>0.1 MeV) at different positions of the 10 rods after the target had received a total of 6.8 A h of proton charge. Using the damage cross-sections calculated by Barnett et al. [11], the corresponding

Table 3
The contents in the specimen rods

Rods with test samples			Rods with fillings			Removable Zircaloy rods and tubes	
No	Test sample type	TC[a]	No	Filling	TC[a]	No	TC[a]
1	Tensile, tear, TEM/SP	2	A	SA 316L		ZR1	1
2	Tensile, tear, TEM/SP		B	CW 316L		ZR2	
3	Bend-fatigue, tensile, TEM/SP		C	F82H		ZR3	
4	Tear, TEM/SP	2	D	9Cr–1Mo		ZR4	
5	Bend-bar, TEM		E	Lead		ZR5	
6	Bend-bar, TEM		F	Lead		ZT1	
7	Charpy		G	Lead		ZT2	
8	Charpy		H	9Cr–1Mo		ZT3	
9	Charpy		I	Lead			
10	Tensile, tear, TEM/SP	2	J	Lead			
			K	316L	1		
			L	Lead			
			M	Lead			

[a] TC: thermocouple.

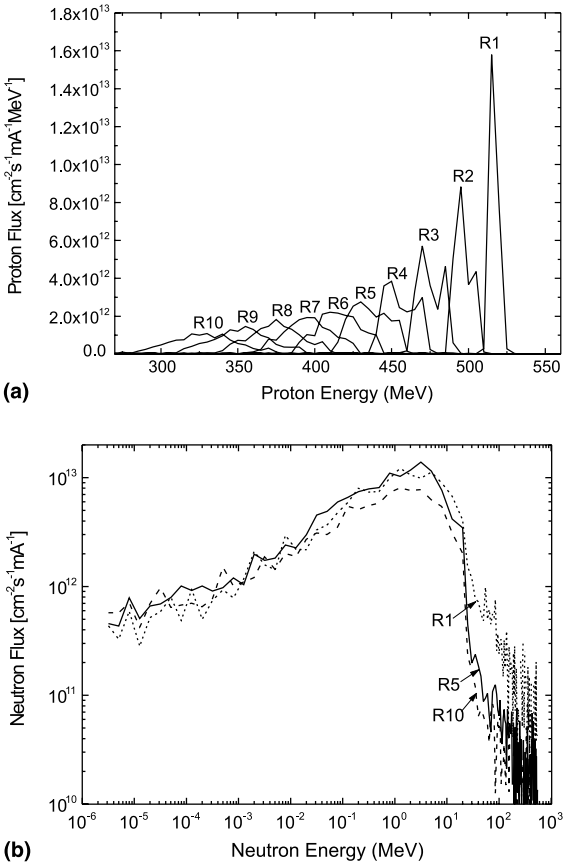

Fig. 8. (a) Proton spectra at the centre position of each specimen rod, (b) neutron spectra at the centre positions of Rods 1, 5, and 10 calculated with the LAHET code.

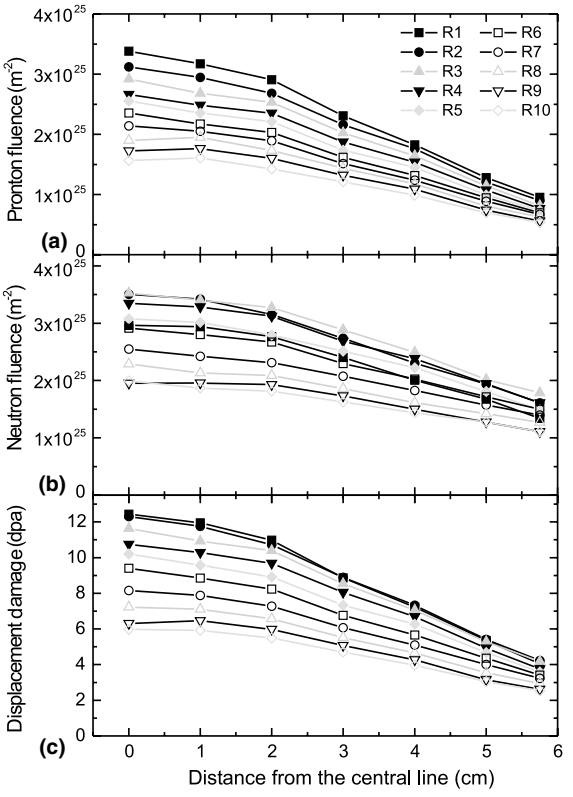

Fig. 9. Calculated proton and neutron fluence distributions and dpa profile along the axial position of each specimen rod.

displacement damage values (dpa) for stainless steel 316 type have been calculated and are presented in Fig. 9(c). It can be seen that the samples were irradiated to a dose range of 2.5–12.5 dpa. Generally protons contributed the main part of the displacement damage. However the spallation neutrons have also significant contributions, whose relative importance increases with the distance from the central line and the depth into the target from about 30% at the centre of Rod 1 to about 50% at the edge of Rod 10.

More detailed calculation will be performed with LAHET and MCNP-X codes to achieve the dpa values and gas (helium and hydrogen) concentration for all the materials included. To verify the calculation results, gamma analysis on the dosimetry discs will be done to obtain the activities of radioactive nuclei produced by protons and neutrons. The measurement results will be analysed with the code named STAYSL2 [12] to assess the proton and neutron spectra at different positions in the target. Furthermore, TEM discs from all the materials will be sent to Pacific Northwest National Laboratory for gas measurements.

5. Irradiation temperature

As mentioned above, there were 6 thermocouples installed in 3 of the 10 specimen rods and 2 thermocouples installed in other rods. The temperatures together with the proton-beam current were normally recorded every minute and could be measured every 5 s if desired. Therefore the history of the irradiation is well documented. Fig. 10 demonstrates how the measured temperatures vary with the beam current at different positions of the specimen rods in the event of beam trips. This sequence is selected for demonstration. Normally the proton beam was stable with an average rate of 1 trip every 30 min.

It can be seen in Fig. 10 that the highest irradiation temperature was about 350°C and lowest temperature was about 70°C at a beam current of about 850 μA. This temperature pattern was kept during the first 13 months of the total 15 months' irradiation. In the last two months, the temperature was increased due to a modification in the main-beam line which resulted in delivering 25% more protons to the target. The temperature range was then from 70°C to 420°C. Unfortunately during the beam tuning after the changes in the beam

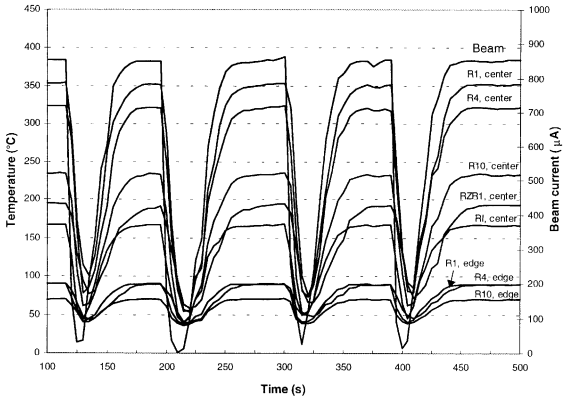

Fig. 10. The measured beam current and temperatures during irradiation. Note that this sequence is selected for demonstrating how the temperatures vary with the beam current. Normally the beam current is nearly constant for much longer time.

line, the target received a very narrow but very high-intensity beam for a very short time (few seconds). The consequence of this will be discussed below.

Fig. 10 shows that the temperature responded almost instantaneously to the proton-beam current. This allows the temperature distribution in the specimen rods to be calculated directly from the energy deposition values obtained from the LAHET calculation.

An effort was made to calculate the temperatures using the ANSYS code [13]. An example is illustrated in Fig. 11 for the situation at the central cross-section of Rod 1 with a proton-beam current of 0.85 mA. Due to the symmetry of the structure only half of the cross-section is shown. The figure presents an idea about the temperature distribution. The maximum calculated temperature at the centre is 334°C, which is in good agreement with the measured value of 350°C (Fig. 10)

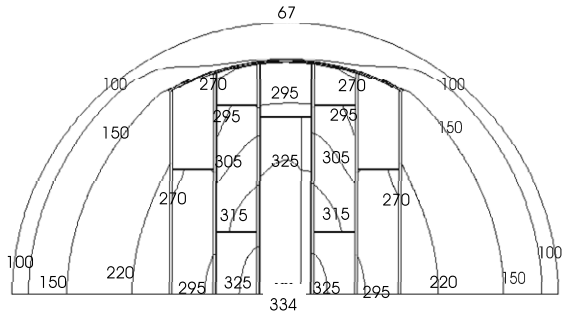

Fig. 11. The calculated temperature distribution at the centre of Rod 1 for a beam current of 0.85 mA, assuming a width of 10 μm for the vertical gaps between the specimens. The numbers indicate the temperature in degrees Celsius.

allowing for the complicated geometry of the system and uncertainties in the calculated heat deposition.

It should be noticed that there are a number of parameters for which values have to be guessed for the calculations. This can lead to large uncertainties. One of the most important parameters is the gap thickness between specimens. With increasing gap thickness the temperature difference between two adjacent specimens increases rapidly, as can be seen from Fig. 11 which holds for the case of 10 μm thickness for the vertical gaps. Since the real thickness of the gaps is not known, the calculation is expected to have 5–10% uncertainty. The calculated temperature of the samples (with rectangular shapes in the middle part) ranges from about 250°C to 350°C.

6. Post-irradiation examination

After irradiation, the target was removed from the target station to a storage port. It was opened in a special hot-cell after cooling down for six months. Photographs taken from the target are shown in Fig. 12(a) for the target safety container and Fig. 12(b) for the target matrix. The black area at the centre of the safety container is a deposit of cracked hydrocarbons and corresponds to the footprint of the proton beam. The irradiated area can also be seen on the target matrix. Some discs were cut out from the proton-beam window of the safety container and preliminary examination was performed. First results have been report elsewhere [14].

All the specimen rods and the other special rods were transported to PSI's standard hot-cell. The first investigation was a γ-scan on all the removed rods. Fig. 13 is an example, showing the results of activity measured from the tube ZT2 which was the located at the centre of the first row in the target (Fig. 7). The data points of the total activity can be perfectly fitted with a Gaussian distribution with $\sigma = 29.8$ mm. This σ value is somewhat lower than the assumed one, 35.6 mm for the proton beam. Further investigation will be performed to find out the cause of this difference.

After the γ-scan the specimen rods were cut near the end and the sample packages were taken out from the tubes. Most of the samples could be easily unloaded from the packages. However, some of the samples could not be separated (Fig. 14). It is clear that some aluminium samples and dosimetry discs had melted during the short-irradiation time with narrow beam size and high intensity mentioned above. The melted aluminium spread into the gaps between specimens, and then stuck the specimens together.

The samples retrieved have been loaded into small specimen containers and are ready to be transported to the different laboratories for examination. The PIE will

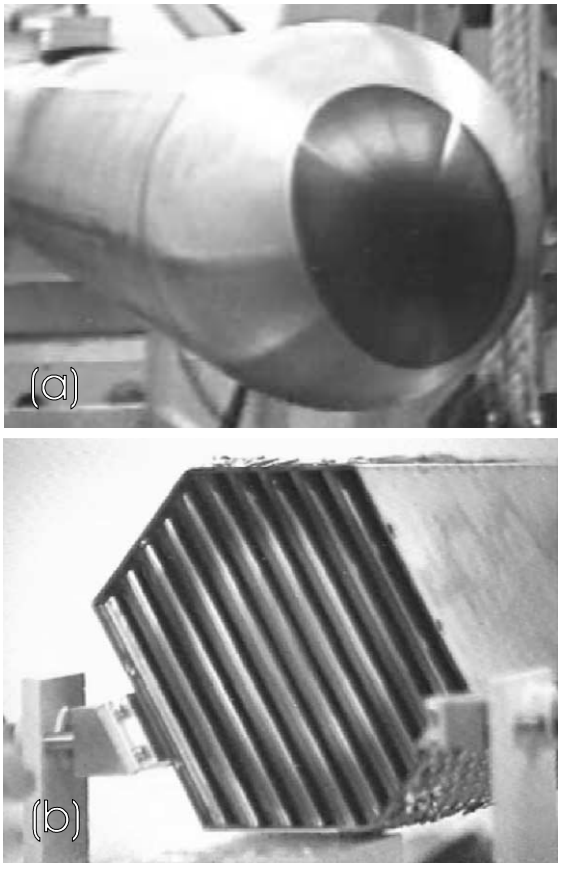

Fig. 12. Photographs show the view of (a) the target safety container and (b) the target matrix after irradiation. The outer diameter of the safety container is 212 mm.

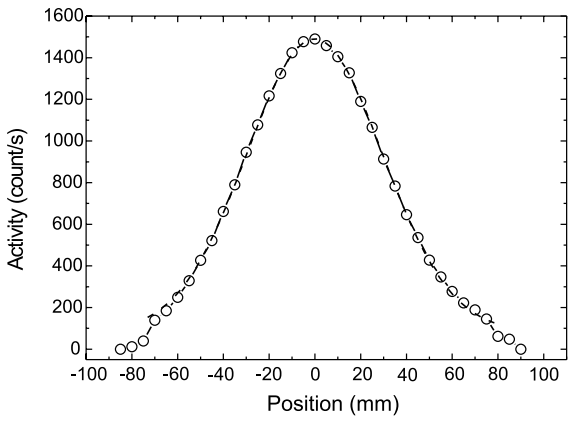

Fig. 13. γ-scan results of Zircaloy-2 tube ZT2 (Fig. 6). The data of the total activity can be fit with a Gaussian distribution of $2\sigma = 59.7$ mm.

Fig. 14. A photograph showing two tear samples stuck together by melted aluminium.

be started soon and the main results should be available in the year 2001.

7. Outlook

In the present SINQ target MARK-III there are another 2080 samples of the similar type under irradiation. This target has been irradiated for one year and received 5.6 A h charge of protons. Because of the reduced beam diameter this gives more or less the same peak proton fluence as received by MARK-II. However the neutron flux is greater than before since the target rods are now Pb clad with steel tubes. The irradiation will be continued for another 7–8 months starting from May 2001. When the irradiation is finished by the end of 2001, the fluence will have almost doubled. This means the samples in the target MARK-III will reach a maximum dose of about 22–25 dpa. The details of the irradiation program in the present target (STIP-II) will be report later elsewhere.

A new irradiation program (STIP-III) has been planned to be performed in the next SINQ target which will be run in the years 2002 and 2003. There, a maximum dose of about 30–35 dpa is anticipated.

Acknowledgements

Dr M. Pepin performed the neutronic calculation and Dr L.P. Ni performed the calculation of temperature distribution. Both of them are greatly acknowledged. The authors would like to thank Mr K. Geissmann for his successful co-ordination of the target construction and also for his temperature measurement data.

References

[1] G.S. Bauer, Y. Dai, PSI Annual Report 1995, Annex-IIIA, p. 3.
[2] Y. Dai, in: Proceedings of Second International Workshop on Spallation Materials Technology, Ancona, Italy, September 18–21, p. 265.
[3] W. Sommer, in: Proceedings of First International Workshop on Spallation Materials Technology, Oak Ridge, April 23–25, 1996, p. 3.2-1.
[4] Y. Dai, in: Proceedings of ICANS-XIII and ESS -PM4, PSI, October 11–19, 1995, p. 604.
[5] L. Mansur, K. Farrell, in: International Workshop on the Technology and Thermal Hydraulics of Heavy Liquid Metals, Schruns, Austria, March 25–28, 1996, p. 6-1.
[6] R.L. Klueh, in: Proceedings of First International Workshop on Spallation Materials Technology, Oak Ridge, April 23–25, 1996, p. 3.3-19.
[7] P. Jung, A. Hishinuma, G.E. Lucas, H. Ullmaier, J. Nucl. Mater. 232 (1996) 186.
[8] Y. Dai, PSI Technical Report, TM-36-98-11.
[9] A. Dementyev, G.S. Bauer, Y. Dai, E. Lehmann, ICANS-XIV, Starved Rock Lodge, USA, June 14–19, 1998.
[10] M. Pepin, private communication.
[11] M.H. Barnett, M.S. Wechsler, D.J. Dudziak, R.K. Corzine, L.A. Charlton, L.K. Mansur, in: Proceedings of Third International Topical Meeting on Nuclear Applications of Accelerator Technology (AccApp99), p. 555.
[12] M.R. James, S.A. Maloy, W.F. Sommer, P.D. Ferguson, M.M. Fowler, G.E. Mueller, R.K. Corzine, in: J.G. Williams, D.W. Vehar, F.H. Ruddy, D.M. Gilliam (Eds.), ASTM STP 1398, American Society for Testing and Materials, West Conshohocken, PA, in press.
[13] L. Ni, G.S. Bauer, PSI Scientific Report 1998, vol. VI, p. 30.
[14] Y. Dai, H. Kaiser, K. Geissmann, G.S. Bauer, R. Zumsteg, H.P. Linder, F. Gröschel, PSI Scientific and Technical Report 2000, vol. VI, p. 33.